S©MR

СИБИРСКИЕ ЭЛЕКТРОННЫЕ
МАТЕМАТИЧЕСКИЕ ИЗВЕСТИЯ
Siberian Electronic Mathematical Reports
http://semr.math.nsc.ru
ISSN 1813-3304

Том 20, № 2, стр. 144–145 (2023) УДК 519.6
https://doi.org/10.33048/semi.2023.20.??? MSC 65M32

ON THE ABERRATIONS CORRECTION IN ULTRASOUND IMAGES IN CASE OF HETEROGENEOUS MEDIA

A.V. VASYUKOV, I.B. PETROV

COMMUNICATED BY ...

Abstract: This paper is devoted to a possible approach to aberrations correction in ultrasound images in case of heterogeneous media. Numerical modeling is performed for a direct problem - obtaining synthetic numerical ultrasound images using known geometry and rheology of the region, as well as transducer parameters. The numerical images reproduce distortions and artifacts that are typical for a medium containing areas with significantly different sound speeds. Convolutional neural networks are used to locate the interface of acoustically contrasting media. The located interfaces between areas with significantly different sound speeds are used to improve the quality of the image. The results of the present work demonstrate that it is possible to improve the quality of images using reasonably fast algorithms based solely on information from the ultrasound sensor. The discussion section of the paper mentions the problems that should be addressed to allow future hardware implementation of the proposed approach.

Keywords: ultrasound, aberration, focusing, matrix probe, numerical modeling, convolutional neural networks.

Vasyukov, A.V., Petrov, I.B., On the aberrations correction in ultrasound images in case of heterogeneous media.

The work was supported by Russian Science Foundation project 22-11-00142.
Received October, 18, 2024, Published ..., .., ...

1 Introduction

This work considers the possibility of correcting aberrations in a medical ultrasound image obtained in a heterogeneous medium containing areas with significantly different sound speeds. This formulation is aimed at further application to the problems of visualizing brain structures through the bones of the skull. Despite the long-term development of medical technology, this particular problem is currently still extremely difficult - existing methods have many limitations and require extremely high qualifications of the specialist conducting the study.

In transcranial ultrasound examination of brain tissue through the skull, the area in which the waves propagate is heterogeneous. The bone tissue of the skull wall has rheological parameters that differ significantly from the parameters of soft tissues. At the same time, typical algorithms of common commercially available equipment are based on the assumption that the speed of sound in the examined area changes slightly. This assumption is appropriate when it comes to soft tissues. However, when examining the brain through the skull, this basic assumption is not met, causing traditional approaches to ultrasound imaging to produce a highly distorted pictures, with artifacts and aberrations appearing in the image [1].

The use of ultrasound for the diagnosis of complex media is an actively researched but very challenging area. The works [2, 3] study the possibility of implementing acoustic tomography. This means solving the inverse problem of reconstructing the density and the speed of sound of the medium. The problem statement of acoustic tomography is very interesting, but extremely computationally challenging. Its formulation is more general and more complex than the one we consider in this paper. We assume to restrict ourselves to the correction of classical medical ultrasound images for the case when they are acquired in a highly heterogeneous environment.

Of the related works, the paper [4] should be especially noted. It demonstrated the possibility of obtaining ultrasound images of point scatterers by compensating for aberrations introduced by cranial bones. The same group studied recently the problem of HIFU focusing through the skull [5]. However, these works rely on the known geometry of the skull wall. Our approach is very similar to the one described in these papers, but we aim to determine the shape of the aberrator from the same ultrasound data that we use for building the image.

In this paper, we consider aberrations in an ultrasound image in the presence of an acoustically contrasting layer and the location of the object of interest beyond the boundary of the media interface. We consider bright point reflectors as the objects of interest, since they can be routinely reproduced on a medical phantom in natural experiments.

This work aims to propose an image correction method that will be able to operate in a near-real-time mode. This will ensure the possibility of its applied use in the future. The approach is based on solving the problem of

localizing the skull wall and subsequently taking its geometry into account when constructing the image.

Convolutional neural networks are considered for skull wall localization. Their choice is due to the rich experience of their use for related biomedical problems and the fact that it is possible to ensure high speed of their operation. Convolutional networks were used for ultrasound problems in [6], the work [7] showed the possibility of their use in elastography problems, and publications [8, 9, 10] present the experience of using convolutional networks specifically for three-dimensional ultrasound data.

2 Mathematical model and numerical method

This paper uses numerical modeling for the direct problem. We consider the ultrasonic pulse propagation in the media to obtain synthetic computed ultrasonic images from the known geometry and rheology of the region, as well as transducer parameters.

The acoustic approximation is used to describe the medium [11]. This model is a significant simplification compared to the full system of elasticity equations, it contains only longitudinal (pressure) waves, there are no transverse (shear) waves in the acoustic approximation. Nevertheless, this approach is widely used to describe ultrasonic pulses in biological tissues, since the attenuation coefficient of shear waves for ultrasound is four orders of magnitude greater than that of longitudinal waves at MHz frequencies [12].

According to the acoustic model, the ultrasound signal propagation is described by the following equations:

$$\rho(\mathbf{x})\frac{\partial \mathbf{v}(\mathbf{x},t)}{\partial t} + \nabla p(\mathbf{x},t) = 0 \qquad \text{in } \Omega, \tag{1}$$

$$\frac{\partial p(\mathbf{x},t)}{\partial t} + \rho(\mathbf{x})c^2(\mathbf{x})\nabla \cdot \mathbf{v}(\mathbf{x},t) = -\alpha(\mathbf{x})c(\mathbf{x})p(\mathbf{x},t) \text{ in } \Omega, \tag{2}$$

where Ω is the computational domain, $\rho(\mathbf{x})$ is the material density, $\mathbf{v}(\mathbf{x},t)$ is the velocity vector, $p(\mathbf{x},t)$ is the acoustic pressure, $c(\mathbf{x})$ is the speed of sound, $\alpha(\mathbf{x})$ is the Maxwell's attenuation coefficient.

The wavefront construction method is used for the numerical solution. The implementation uses the modifications described in [1]. This numerical method is focused exclusively on acoustic equations, which is an acceptable limitation for the present work. The method was demonstrated to provide numerical ultrasound images that match the experimental data qualitatively and quantitatively. The method allows one to describe the reflection from long boundaries and from point reflectors. The boundary between the layers and the boundaries of large pores are described using long boundaries approach. The small reflectors are considered as point ones. Signal processing and B-scan image generation follow the algorithms described in [13].

The transducer is a matrix phased array that is located on the border of the area under examination. It is modeled as a set of border conditions with

a given dependency of pressure versus time. The signal from a single element of array is described by the following formula:

$$\sigma_{zz}^{border} = P \cdot e^{-(t-t_0)^2/2t_{pulse}^2} \cdot \cos(\omega(t-t_0)), t > t_0;$$
$$\sigma_{zz}^{border} = 0, t < t_0,$$

where t is the current time, t_0 is the starting time of the signal (which is used to model the delay for the phased array), σ_{zz}^{border} is the corresponding stress tensor component on the border node, P is the maximum amplitude of the wavefront, parameter ω is the carrier frequency, parameter t_{pulse} corresponds to the width of the pulse.

The first step of the aberration correction within the framework of this work is to determine the shape of the interface between acoustically contrasting layers. The input data for solving the inverse problem is the response from the medium registered by the matrix ultrasonic sensor. The output data of the inverse problem is the position of the interface between two media. Convolutional neural networks are used to solve this inverse problem.

To train the neural networks, a synthetic data set was formed from the results of 1024 calculations of the direct problem. The calculations varied the position and shape of the acoustic contrast layer, the number and position of large pores in the model skull wall, and the number and position of small bright reflectors in the tissues forming the background signal. Separately prepared examples were used for testing neural networks, these samples were not included in the training set.

In this paper, 2D and 3D networks are used in order to compare the results. All convolutional networks follow the common UNet architecture [14]. The depth of both 2D and 3D networks was 4 blocks. In the case of 2D network, the volume of three-dimensional data is represented as a set of two-dimensional slices [15]. When processing each slice, three channels are presented to the network input - the target slice and two neighboring ones, which to some extent allows the network to obtain information about the three-dimensional environment of objects on the slice. In the case of 3D network, 3D data is given as input, and a patch-based approach [16, 17] is used as it allows flexibility in managing the RAM requirements on the GPU when processing large size input data. The parameters of 3D network are presented in the Table 1.

3 Numerical results

First, the convolutional network is trained to detect the boundary between acoustically contrast layers.

The direct problem for this stage involves the calculation of ultrasonic signal propagation in a region containing the boundary between acoustically contrasting layers. The calculation region is a parallelepiped. The upper edge of the parallelepiped corresponds to the outer boundary of the region, in the center of which the matrix ultrasonic sensor is located. Outside the area of

Table 1. Hyperparameters for 3D neural network

Parameter	Value
Activation	ReLU
Normalization	Batch
Convolution kernel size	3
Convolution kernel stride	1
Convolution type	same (middle)
Number of blocks	4
Input tensor size	16x16x512
Output tensor size	16x16x512
Input channels	1
Output channels	1

contact with the transducer, the upper edge is modeled as a free surface. The external pressure profile is defined in the transducer location region. A non-reflective boundary condition is set for the other three boundaries of the computational domain.

It is assumed that the boundary between the two acoustically contrasting layers is smooth and can have an arbitrary shape. In addition, the upper layer contains many small reflectors that create background noise in the final ultrasound image, as well as a number of large pores, the response from which is comparable in intensity to the reflection from the boundary between the layers.

The speed of sound in both layers is constant. The upper layer is harder and the speed of sound in it is assumed to be 3.0 km/s. The lower layer is softer, with a sound velocity of 1.5 km/s. The number of small reflectors in the calculations varied from 100 to 2500. The number of large pores varies from 5 to 50.

When training a neural network, the matrix sensor has a square shape of 24x24 elements. The sensor emits a signal with a frequency of 3 MHz. The sampling frequency at signal receive is 45 MHz. The final dimensionality of the received data is 24x24x1024. Here 24x24 is the physical dimensions of the sensor, and 1024 is the number of time samples recorded during the experiment by each sensor element.

Figure 1 shows the interface profile in one of the calculations. Four slices of full three-dimensional data are shown - the position of the boundary under the rows of sensor elements from the 5th to the 8th. On the vertical axis are the 24 matrix sensor elements in a given slice. On the horizontal axis - time samples. In the figure the image is cropped to the first 400 samples from the full set of 1024 samples.

Figure 2 shows the unprocessed ultrasound image for this calculation. The overall noise, which is visually seen as fluctuations in the gray background intensity, is due to the large number of small reflectors in the medium. The interface is visible as a region of intense response of variable amplitude.

Individual bright responses from large pores at depths of 50, 70, 90, 110, 130, and especially 230 (the last two slices in the figure) are visible. These bright responses especially strongly interfere with the automatic image processing, as they even exceed in intensity the response from the desired boundary.

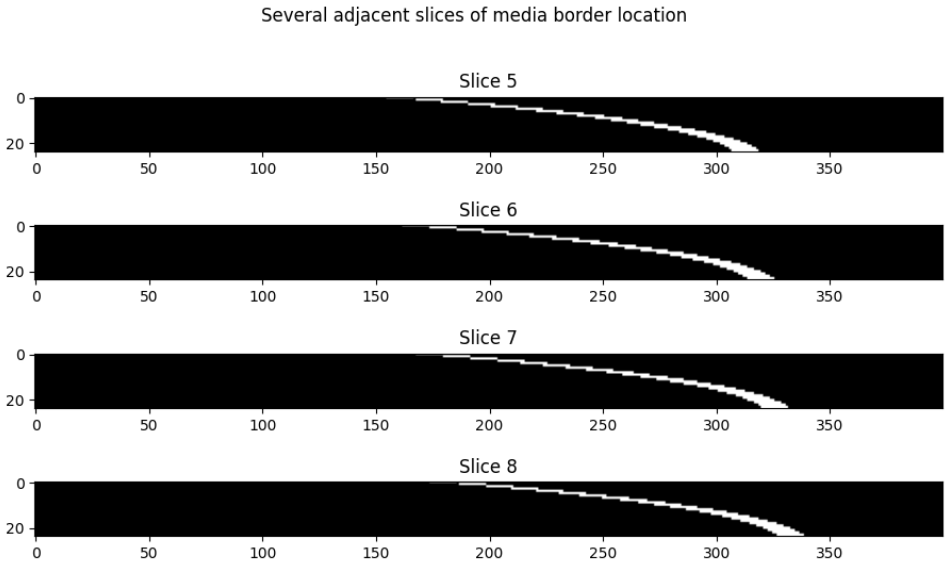

FIG. 1. Boundary location

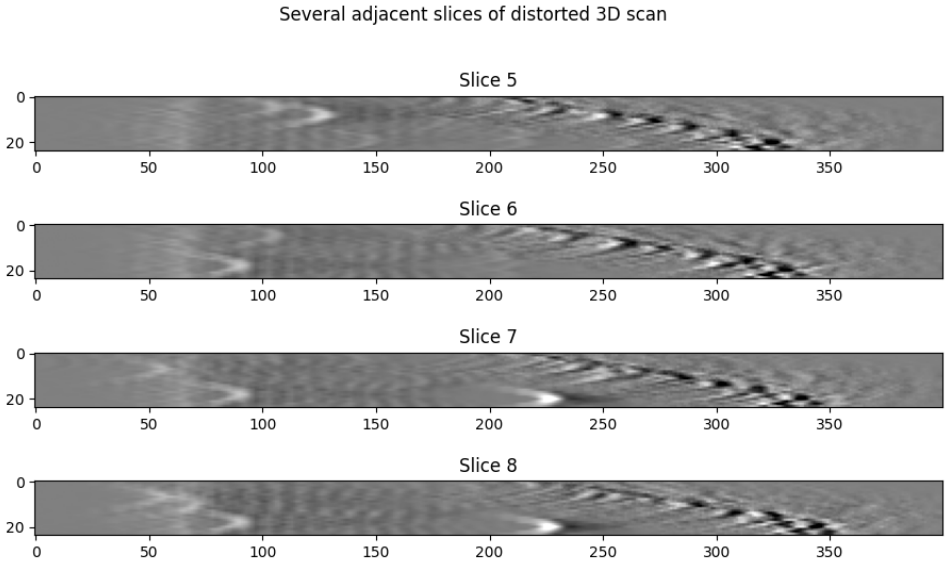

FIG. 2. Unprocessed B-scan

Figures 3 and 4 show the results of the convolutional networks of 2D and 3D structure.

One can see that the boundary is correctly located in both scenarios, but its blurring is significantly less for the 3D network. It is worth noting that the 3D network is almost unaffected by noise and interference in the input signal, both random and caused by the presence of large bright reflectors. The 2D network results show a significant number of borders identified in the region before the desired boundary - where the large pores are located. This is not any random error - the network is solving a segmentation problem to detect acoustically contrasting boundaries, and pore boundaries also fall into this category. However, this effect is undesirable. With the 3D network, problems of this nature are virtually eliminated. This is because the 3D structure of the input data allows the convolutional network to fully utilize the spatial information about the reflectors and to learn to ignore geometrically small objects. The total execution time of all operations on a single 3D image using the 3D network was about 0.1 seconds on commercially available graphics cards.

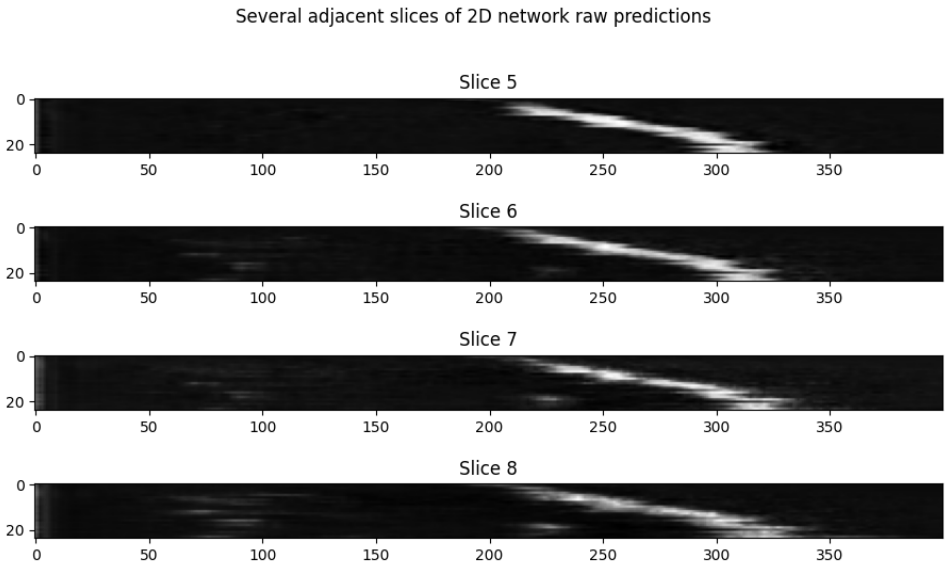

FIG. 3. Prediction of 2D network

It was noted above that a patch-based approach was used for 3D network, the input was a tensor of dimension 16x16x512. This allows us to expect that it is possible to transfer the trained network to a sensor of a different geometry while maintaining the sampling rate and distance between neighboring sensor elements. To test this hypothesis, further experiments on aberration correction were performed for a sensor of 32x32 elements.

Different approaches can be used to correct aberrations. We used the following sequence of operations.

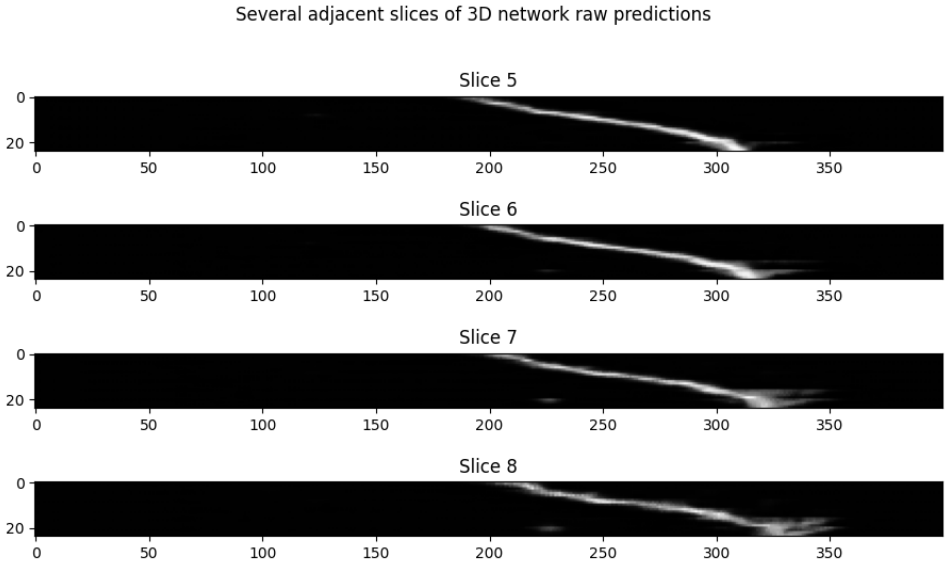

FIG. 4. Prediction of 3D network

(1) A preliminary ultrasound image is formed using delay and sum beamforming. At this stage, a fixed sound velocity of 1500 m/s is used, which is typical for soft tissue. This image is fully subject to aberrations in the region behind the acoustically contrast prism.
(2) The preliminary image is used to determine the geometry and position of the aberrator. The convolutional network is used for this stage as described above. The input of the neural network is the preliminary image. The output is the position of the two aberrator boundaries – front and back.
(3) The resulting aberrator shape is used to form the final image. A simple delay and sum beamforming is applied again, but it is corrected to take into account that the signal in the medium propagates in two regions with different sound velocities. This allows compensating the phase difference on the elements of the phased array and restoring the quality of focusing behind the acoustically contrast prism.

An example of how such an algorithm works is presented below. Figure 5 shows an image of a medium with three bright small reflectors obtained without an aberrator. The three model reflectors are clearly distinguishable. Figure 6 shows an image obtained for the same medium when scanning through an aberrator. The sound velocity in the main volume of the medium is 1500 m/s, in the prism – 3000 m/s. It can be seen that in this case the difference in travel time introduced by the aberrator leads to a significant blurring of the images of reflectors. The effect is especially pronounced for the leftmost reflector, which is closest to the prism. Its image becomes faintly distinguishable even for this ideal test case. In a real problem statement,

where background noise is inevitably present, it is likely that this reflector would become completely indistinguishable against the overall gray background of the ultrasound image. Figure 7 shows the result of image correction using the proposed approach. It can be seen that the image quality of all reflectors is significantly improved.

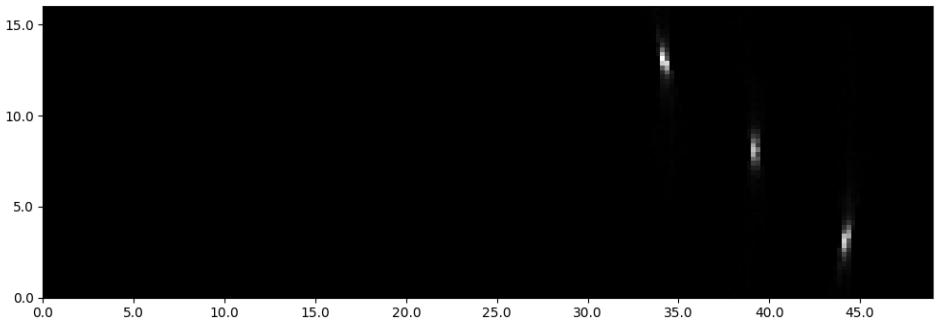

FIG. 5. Results of scanning without aberrator

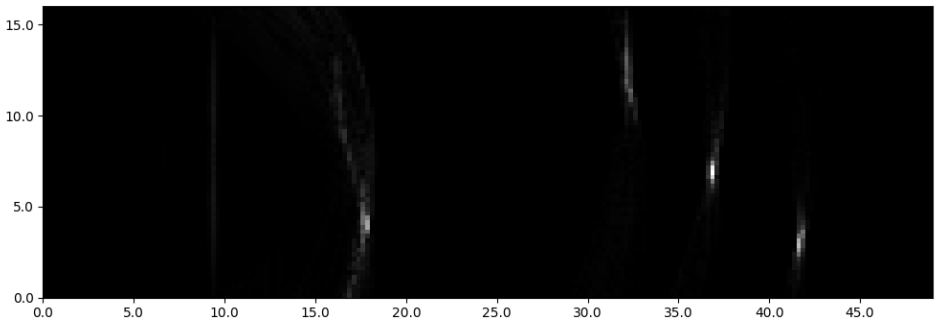

FIG. 6. Results of scanning with aberrator

4 Discussion and concluding remarks

The results of the present work demonstrate that it is possible to improve the quality of ultrasound images in the case of heterogeneous medium using reasonably fast algorithms based solely on information from the ultrasound transducer.

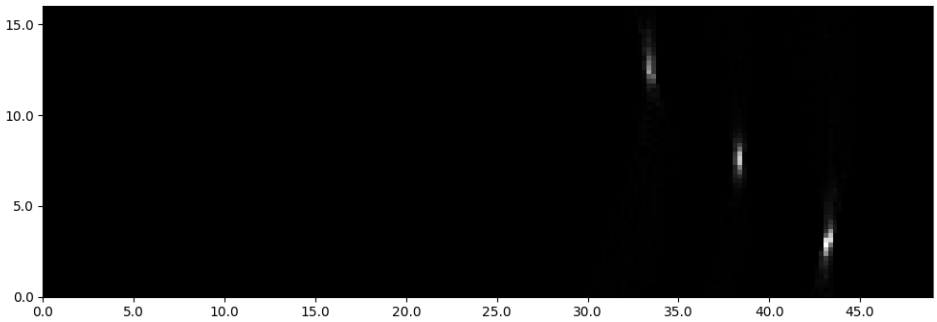

Fig. 7. Results of scanning with aberrator and correction applied

It should be noted that the effectiveness of the proposed approach depends on a number of factors.

Preliminary image formation is based on the assumption that the aberrator boundaries are smooth enough and oriented in such a way that they reflect a significant part of the signal energy in the direction of the sensor. This assumption seems to be acceptable for the target problem, since in reality the wall of the human skull is exactly like this at any reasonable orientation of the sensor. Nevertheless, this point must be taken into account if the same approach is to be transferred to other areas where contrast inclusions may have a less convenient shape.

Formation of the final image strongly depends on the quality of aberrator shape detection. If its boundaries are poorly defined, the correction of the phase difference will not be sufficient. This limitation again seems to be acceptable, because in case of bad correction the final image will not contain any «hallucinations», but simply will be blurred, which is easily noticeable visually. At the same time, a small change in the sensor position will result in a change in the input data for determining the shape of the aberrator, which will give a new result for localizing its boundaries. Thus, in a few movements of the sensor, it is possible to find a position in which the quality of the aberrator identification is sufficient to obtain good focusing.

Generally speaking, using delay and sum beamforming with correction only for the speed of sound in the medium is not an accurate approach. Such an algorithm assumes that the shortest path from the phased array element to the reflector in the medium is a rectilinear signal propagation. However, when there is a large difference in the sound velocities in the two regions, and the geometry of the regions is complex, the shortest path may not be rectilinear. The phase correction in the proposed approach takes into account the differences in sound velocity in the two materials, but does not take into account the differences in the path from a straight line. This explains the

incomplete compensation of aberrations in figure 7 compared to figure 5. Nevertheless, this approximation allows to obtain a good image correction using a simple algorithm with low computational costs.

The results of this work can be used to create new algorithms for constructing ultrasound images using methods for compensating distortions caused by differences in sound velocities in tissues. However, it should be noted that an implementation of the proposed approach may be difficult in real life. Typical ultrasound equipment does not provide an access to raw data from the elements of the phased array. The processing of individual elements data occurs inside the sensor. Only the formed image is transferred to the host system and available programmatically. That is, the hardware implementation of the proposed approach will require significant engineering work in any case – either it will be necessary to transfer a different set of data to the host system, or to implement the entire proposed algorithm inside the sensor. Therefore, practical implementation of the proposed ideas requires further work.

References

[1] K.A. Beklemysheva, G.K. Grigoriev, N.S. Kulberg, I.B. Petrov, A.V. Vasyukov, Y.V. Vassilevski, *Numerical simulation of aberrated medical ultrasound signals*, Russian Journal of Numerical Analysis and Mathematical Modelling, **33**:5 (2018), 277–288.

[2] M.A. Shishlenin, N.A. Savchenko, N.S. Novikov, D.V. Klyuchinskiy, *On the reconstruction of the absorption coefficient for the 2D acoustic system*, Siberian Electronic Mathematical Reports, **20**:2 (2023), 1474–1489.

[3] S.I. Kabanikhin, D.V. Klyuchinskiy, N.S. Novikov, M.A. Shishlenin, *Numerics of acoustical 2D tomography based on the conservation laws*, Journal of Inverse and Ill-posed Problems, **28**:2 (2020), 287–297.

[4] D.A. Sukhoruchkin, P.V. Yuldashev, S.A. Tsysar, V.A. Khokhlova, V.D. Svet, O.A. Sapozhnikov, *Use of Pulse-Echo Ultrasound Imaging in Transcranial Diagnostics of Brain Structures*, Bulletin of the Russian Academy of Sciences: Physics, **82**:5 (2018), 507–511.

[5] D.D. Chupova, P.B. Rosnitskiy, O.V. Solontsov, L.R. Gavrilov, V.E. Sinitsyn, E.A. Mershina, O.A. Sapozhnikov, V.A. Khokhlova, *Compensation for Aberrations When Focusing Ultrasound Through the Skull Based on CT and MRI Data*, Acoustical Physics, **70** (2024), 288–298.

[6] D. Perdios, M. Vonlanthen, F. Martinez, M. Arditi, J.-P. Thiran, *Single-shot CNN-based ultrasound imaging with sparse linear arrays*, 2020 IEEE International Ultrasonics Symposium (IUS), Las Vegas (2020), 1–4.

[7] D. Patel, R. Tibrewala, A. Vega, L. Dong, N. Hugenberg, A. Oberai, *Circumventing the solution of inverse problems in mechanics through deep learning: Application to elasticity imaging*, Computer Methods in Applied Mechanics and Engineering, **353** (2019), 448–466.

[8] H. Lu, H. Wang, Q. Zhang, S. Yoon, D. Won, *A 3D Convolutional Neural Network for Volumetric Image Semantic Segmentation*, Procedia Manufacturing, **39** (2019), 422–428.

[9] B. Potocnik, M. Savc, *Deeply-Supervised 3D Convolutional Neural Networks for Automated Ovary and Follicle Detection from Ultrasound Volumes*, Applied Sciences, **12**:3 (2022), article number 1246.

[10] K. Brown, J. Dormer, B. Fei, K. Hoyt, *Deep 3D convolutional neural networks for fast super-resolution ultrasound imaging*, Proceedings SPIE Int Soc Opt Eng, Medical Imaging 2019: Ultrasonic Imaging and Tomography, **10955** (2019), article number 1095502.

[11] T.D. Mast, L.M. Hinkelman, L.A. Metlay, M.J. Orr, R.C. Waag, *Simulation of ultrasonic pulse propagation, distortion, and attenuation in the human chest wall*, The Journal of the Acoustical Society of America, **106**:6 (1999), 3665–3677.

[12] E.L. Madsen, H.J. Sathoff, J.A. Zagzebski, *Ultrasonic shear wave properties of soft tissues and tissuelike materials*, The Journal of the Acoustical Society of America, **74**:5 (1983), 1346–1355.

[13] Y.V. Vassilevski, K.A. Beklemysheva, G.K. Grigoriev, N.S. Kulberg, I.B. Petrov, A.V. Vasyukov, *Numerical modelling of medical ultrasound: phantom-based verification* , Russian Journal of Numerical Analysis and Mathematical Modelling, **32**:5 (2017), 339–346.

[14] O. Ronneberger, P. Fischer, T. Brox, *U-Net: Convolutional Networks for Biomedical Image Segmentation*, Lecture Notes in Computer Science, **9351** (2015), 234–241.

[15] O. Paserin, K. Mulpuri, A. Cooper, R. Abugharbieh, A. Hodgson, *Improving 3D Ultrasound Scan Adequacy Classification Using a Three-Slice Convolutional Neural Network Architecture*, EPiC Series in Health Sciences, **2** (2018), 152–156.

[16] K. Ghimire, Q. Chen, X. Feng, *Patch-Based 3D UNet for Head and Neck Tumor Segmentation with an Ensemble of Conventional and Dilated Convolutions*, Lecture Notes in Computer Science, **12603** (2021), 78–84.

[17] P. Coupeau, J.-B. Fasquel, E. Mazerand, P. Menei, C.N. Montero-Menei, M. Dinomais, *Patch-based 3D U-Net and transfer learning for longitudinal piglet brain segmentation on MRI*, Computer Methods and Programs in Biomedicine, **214** (2022), article number 106563.

Alexey Viktorovich Vasyukov
Moscow Institute of Physics and Technology,
Institutsky lane, 9,
141700, Dolgoprudny, Russia
Email address: vasyukov.av@mipt.ru

Igor Borisovich Petrov
Moscow Institute of Physics and Technology,
Institutsky lane, 9,
141700, Dolgoprudny, Russia
Email address: petrov@mipt.ru